OpenMARS MY34-35 reference manual

Dataset summary

This dataset contains our analysis of the global atmospheric state of Mars over the specified time period through a synthesis of the Mars Global Circulation Model (GCM) used at the Open University and observational data taken by the Mars Climate Sounder (MCS), Nadir and Occultation for Mars Discovery (NOMAD) and Atmospheric Chemistry Suite (ACS) instruments in orbit around Mars. This product is useful as a reference global Martian atmosphere that has been constrained by observations, and for several different studies related to the Martian atmospheric structure.

For any queries on the dataset, please contact: openmars@open.ac.uk

Accessing the dataset

Along with the data files that make up this dataset, there is also a sample Python script that shows an interested user how the data in the files can be easily accessed. The plot that will be created if the supplied Python script (sample_data_plot.py) is run without modification will be identical to the plot shown in Figure 1. The supplied sample Python script can be modified to produce various plots of the different variables stored in the dataset (for some examples of the different plots available, a good place to start is to have a browse at https://matplotlib.org/stable/gallery/index.html).

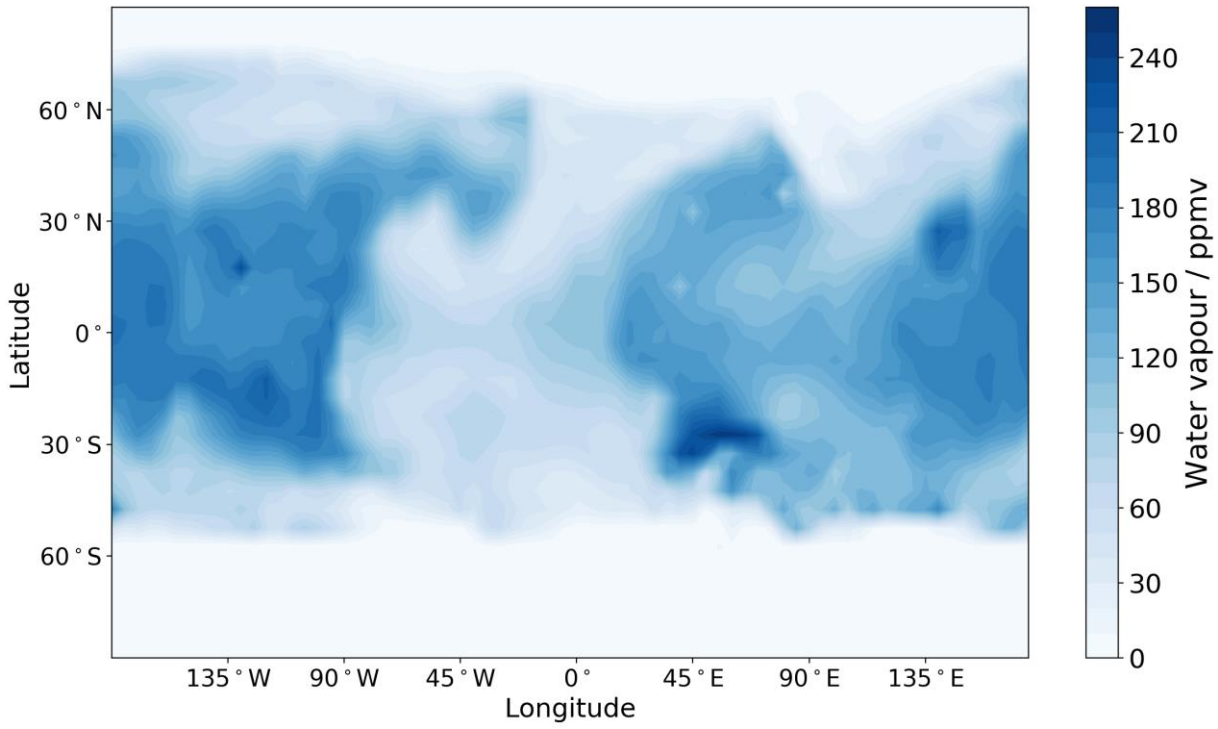

Figure 1 - Sample output of the water vapour volume mixing ratio in the eleventh layer of the atmosphere from the dataset created using the sample_data_plot.py script.

Structure of the reanalysis data files

This section details the structure of the files from the reanalysis which are made publicly available to interested users.

Dataset description

The reanalysis produced for this dataset covers almost half a complete Mars year (coinciding with the primary science phase of the ExoMars Trace Gas Orbiter mission), with any particular data file covering 30 sols. The data files are provided in netCDF4 format which are easily accessible by Python (see sample_data_plot.py for an example of how to access the data). The filename convention is as follows:

openmars_myMM_lsL_myMM_lsL.nc

where MM (34) indicate the Mars Year (MY) and L (0 to 359) the start/end value of solar longitude (to the nearest integer) for the period covered by the data file.

Dimensions

The dimensions of the reanalysis data files are listed in Table 1. The surface and atmospheric reanalysis output in the data files depend on three (longitude, latitude, time) and four dimensions (longitude, latitude, level, time) respectively, with one exception being the visible column dust optical depth which depends on only three (longitude, latitude, time) dimensions. The horizontal grid spacing is 5˚ in both longitude and latitude, with four-dimensional atmospheric variables defined on model sigma levels σ (where $\sigma = p/p_s$, p is atmospheric pressure and p_s is surface pressure) that are non-dimensional terrain-following levels. There are 70 vertical levels in this reanalysis data product extending to an altitude of around 105 km.

Table 1 - Dimensions used for variables in the reanalysis data files.

Dimension	Number of values	Description
lon	72	Longitude
lat	36	Latitude
lev	70	Vertical level
time	720	Time

The primary time variable used for each data file is the Martian sol (see Table 2 for all time variables). For ease of conversion and since the majority of the Mars science community use solar longitude and Mars year, these values are also included. The surface and atmospheric variables are output every 1 Martian hour starting at 1 a.m. on sol 7021 (sol 331 of MY 34), with sol 0 corresponding to $L_S = 0^\circ$ MY 24.

Table 2 - One-dimensional variables in each reanalysis data file.

Variable	Dimension	Description	Units
lon	lon	Longitude	Degrees east
lat	lat	Latitude	Degrees north
lev	lev	Model sigma level	NU
time	time	Martian Sol	Sols since 0.0
Ls	time	Solar longitude	Degrees
MY	time	Mars Year	NU

Surface variables

The surface variables included in each reanalysis data file are listed in Table 3. Although only the surface pressure is included in the reanalysis data files, the atmospheric pressure can be calculated for each vertical level of the atmosphere by multiplying the surface pressure variable ps by the corresponding sigma value of each vertical level in lev.

Although none of the surface variables are directly assimilated in the reanalysis product, each one is altered indirectly as a result of the assimilation of temperature profiles and column dust optical depth.

Table 3 - Surface variables in each reanalysis data file.

Variable	Dimension	Description	Units
ps	lon, lat, time	Surface pressure	Pa
tsurf	lon, lat ,time	Surface temperature	K
co2ice	lon, lat, time	Surface CO_2 ice	kg m^{-2}

Atmospheric variables

The atmospheric variables included in each reanalysis data file are listed in Table 4. As previously mentioned, as the variables dustcol and vapcol are column values it only has three dimensions whereas the other atmospheric variables are all four-dimensional. The zonal wind u and meridional wind v are positive in the eastward and northward direction respectively. Although not directly assimilated, u and v are both indirectly altered as a result of the assimilation procedure.

Table 4 - Atmospheric variables in each reanalysis data file.

Variable	Dimension	Description	Units
dustcol	lon, lat, time	Visible column dust optical depth	NU
temp	lon, lat, lev, time	Atmospheric temperature	K
u	lon, lat, lev, time	Zonal wind (Eastward)	ms^{-1}
v	lon, lat, lev, time	Meridional wind (Northward)	ms^{-1}
vapcol	lon, lat, time	Water vapour column abundance	kg m^{-2}
vmr_h2ovap	lon, lat, lev, time	Water vapour volume mixing ratio	ppmv

Overview of the components used to create the dataset

This section gives an overview of the three different components used to create the OpenMARS dataset, namely the Mars GCM, MCS observational data and the Data assimilation scheme that combines the two sources of information.

Mars GCM

The GCM used to produce this reanalysis product is the Mars Planetary Climate Model (PCM) – UK Spectral (hereafter MGCM), which has been developed in a collaboration of the Laboratoire de

Météorologie Dynamique, the Open University, the University of Oxford and the Instituto de Astrofisica de Andalucia. This model uses physical parameterisations shared with the Mars PCM, which are coupled to a UK-only spectral dynamical core alongside an energy and angular momentum conserving vertical finite-difference scheme. Tracers such as CO_2 and dust are transported by a UK-only semi-Lagrangian advection scheme (Newman et al., 2002) with mass conservation (Priestley, 1993).

The MGCM is similar to the model used in Montabone et al. (2014) for a previous reanalysis dataset but now includes additional sub-models. CO_2 is now transported as an additional tracer providing a better representation of the CO_2 cycle. A thermal plume model is used to better represent turbulent structures in the planetary boundary layer (Colaïtis et al., 2013), of importance for the evolution of tracers. A `semi-interactive' two-moment scheme is used to freely transport dust in the model (Madeleine et al., 2011), although the dust column optical depth at each grid point is scaled to match the observed dust distribution which is assimilated into the MGCM from spacecraft observations. Specific physical parameterisations linked to the water cycle include the cloud microphysics package (Navarro et al., 2014) that accounts for nucleation on dust particles and supersaturation.

The MGCM is also coupled to the LMD photochemical module (Lefèvre et al., 2004). The photochemical module provides multiple photolytic and chemical reactions with up-to-date reaction rates between 16 advected species including carbon dioxide, water vapour and ozone. It also includes heterogeneous processes removing odd hydrogen radicals, a process which has been shown to improve the agreement between models and observations (Lefèvre et al., 2008). Time-varying dust amounts are also taken into account in the photolytic reactions.

The model is truncated at wavenumber 31 resulting in a 5˚ physical longitude-latitude grid (and 3.75˚ longitude-latitude grid for the dynamical core) with 70 vertical levels extending to an altitude of ~105 km. The time-stepping regime for the physical and dynamical parts of the MGCM is 12 and 1.2 minutes respectively.

MCS observational data

This section describes the observations available from the MCS instrument aboard the Mars Reconnaissance Orbiter (MRO) spacecraft. The MCS instrument employs a nearly continuous limb viewing strategy in order to achieve greatly increased sensitivity to minor and trace constituents (McCleese et al., 2007). The instrument is a passive radiometer which retrieves in 9 spectral bands covering the visible and mid- to far-infrared channels. It is capable of retrieving vertical profiles of water ice and dust opacity alongside temperature profiles with a greater vertical resolution than TES (5 km for MCS as opposed to ~10 km). The vertical coverage of the profiles is from the surface up to altitudes of ~85 km (as opposed to ~40 km for TES). The MCS observations comprise two sets of twelve narrow strips of data, separated by ~30° in longitude, a similar pattern to that observed by the TES instrument. Due to the Sun-synchronous orbit of MRO, the MCS observations away from the pole occur at local times around 3 a.m. and 3 p.m., though the actual local time of an observation varies with both latitude and season. The instrument began its coverage of Mars on 24th September 2006 (or L_S = 111° MY 28), in the primary science phase of the mission.

MCS temperature profiles

The retrieval of vertical temperature profiles from the MCS measured radiance is extensively covered in Kleinböhl et al. (2009) and briefly detailed in this section. It uses 3 channels of the MCS instrument (A1-3) in the far-infrared. The radiative transfer equation is inverted to determine the temperature from the radiance using an iterative method. For this process, a ‘first guess’ is needed

for the temperature profile, although the success of this retrieval method is shown to be insensitive to this initial guess (Kleinböhl et al., 2009). The algorithm is processed for each limb profile with 30 iterations, to converge on the final vertical profile of temperature. The error on the retrieval is reduced in the lower atmosphere (0.5 K) and increases at higher altitudes due to the reduction in signal-to-noise ratio (> 1 K above 40 km) and in situations where the atmosphere is opaque. This reanalysis includes improvements based on corrections in lateral temperature gradients through two-dimensional radiative transfer methods providing improved retrievals close to the poles (Kleinböhl et al., 2017). Version 5.2 of the MCS temperature profiles are used in this reanalysis, except during the global dust storm time period in which a re-processed v5.3.2 version that incorporates additional information from the far infrared channel centred at 316 cm^{-1} is included (Kleinböhl et al., 2020).

Figure 2 displays the number of MCS temperature profiles that are assimilated into the MGCM to form part of the final reanalysis product.

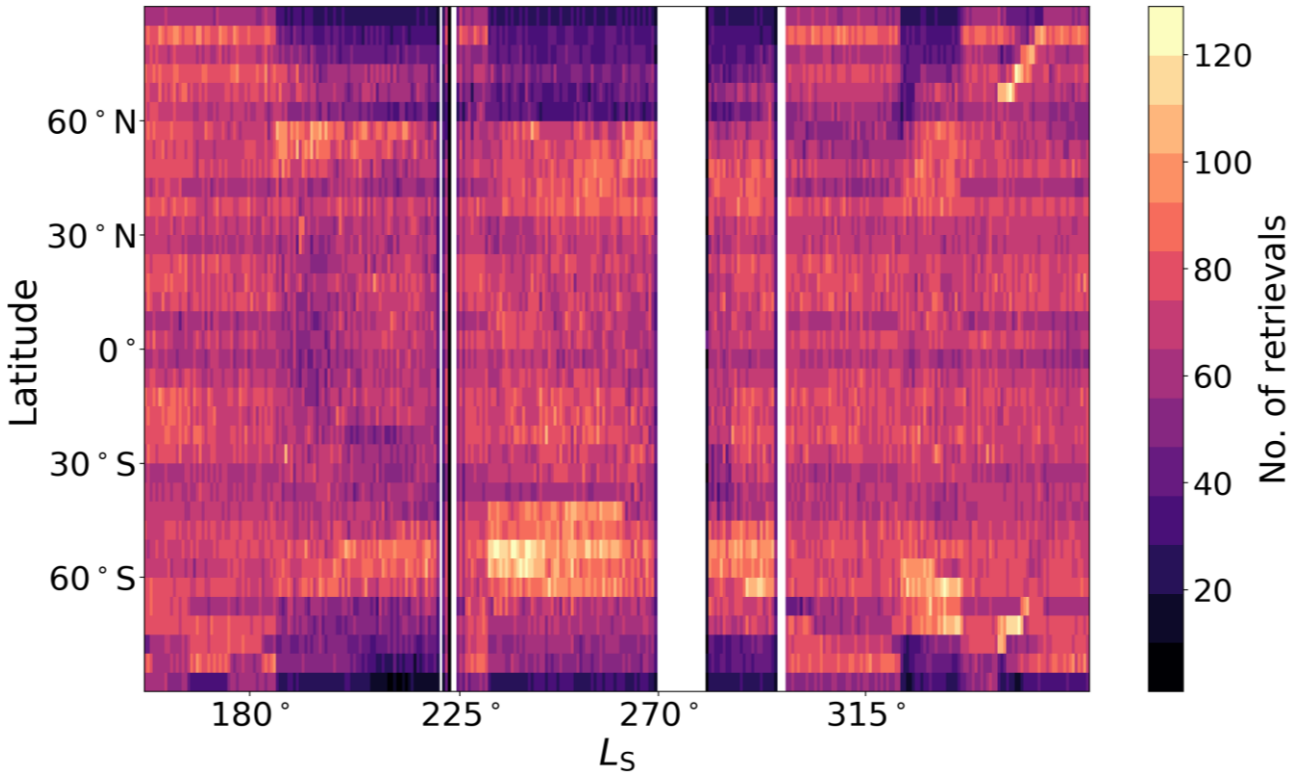

Figure 2 - Number of MCS temperature profiles in 1 sol by 5˚ latitude bins. White indicates no data available in this particular bin.

MCS dust opacity retrievals

The retrieval of dust opacity profiles from the MCS measured radiance is also extensively covered in Kleinböhl et al. (2009). Details of how the column dust optical depth is retrieved are presented in Montabone et al. (2015) and briefly detailed here. For any given successful limb retrieval, the full profile of dust extinction opacity produced by the retrieval algorithm (MCS retrievals from version v5.2 are used for this reanalysis) is integrated to produce a column dust optical depth. The profile is extended upward and downward under the assumption of well mixed dust, based on the last valid value.

The MCS dust profiles cannot be retrieved down to the surface using only limb observations, and the dust in the un-retrieved part of the profile can potentially account for a significant fraction of the total dust column. Therefore estimates of column dust optical depth from MCS observations are likely to introduce errors attributable to either the extrapolation to the surface under the well mixed assumption or the use of dust opacity values at altitudes where the fit to observed radiances is not within the standard threshold.

Figure 3 displays the number of MCS column dust optical depth retrievals that are assimilated into the MGCM to form part of the final reanalysis product. The retrieval method allows for a reliable measurement of dust optical depth during the daytime and nighttime during polar winter over this time period.

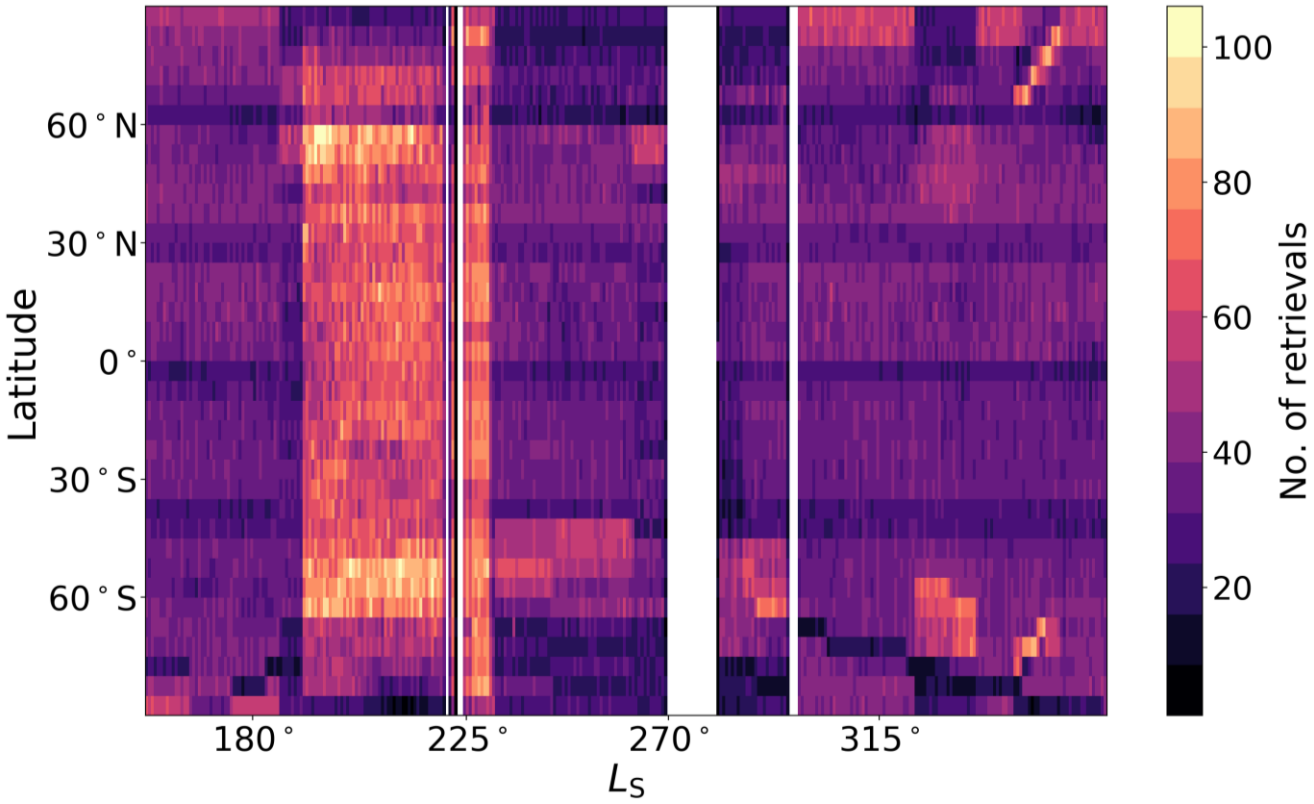

Figure 3 - Number of retrievals of MCS column dust optical depth in 1 sol by 5˚ latitude bins. White indicates no data available in this particular bin.

Quality control

The quality control applied to the MCS temperature profiles is largely described in Lewis et al. (2007). Profiles marked as bad by the retrieval algorithm are automatically rejected, with remaining retrievals filtered to set any temperatures that drop below the CO_2 condensation temperature to be at the CO_2 condensation temperature. After quality control, around 735,000 temperature profiles retrieved by the MCS instrument are available for assimilation into the MGCM.

Quality control for the derived MCS column dust optical depth retrievals is fully described in Montabone et al. (2015) and briefly detailed here. Estimates of the MCS column dust optical depth can be fairly inaccurate if the lowest retrieved level of dust opacity is above ~20 km altitude, depending on the time of the year and the dust/water ice conditions. The dataset therefore largely consists of nighttime retrievals that correspond to dust extinction profiles with valid values at or below 25 km altitude, and only retrievals with local times between 12 p.m. and 6 p.m. when the corresponding extinction profile has valid values at or below 8 km altitude are accepted. Finally,

estimates of column dust optical depth where the temperature profile dropped below the condensation temperature of carbon dioxide at some pressure levels are rejected, because CO_2 ice opacity is currently not taken into account in the retrieval algorithm but can affect retrievals of dust opacity at those levels. During the time period covered by the MCS instrument, around 445,000 column dust optical depth retrievals are assimilated into the MGCM to produce the final reanalysis product.

TGO (NOMAD and ACS) observational data

This section describes the observations available from the NOMAD and ACS instruments aboard the ExoMars Trace Gas Orbiter (TGO) spacecraft. The ExoMars TGO spacecraft, a joint collaboration between the European and Russian space agencies, entered into orbit around Mars on 19th October 2016 and began science operations on 21st April 2018 after a long period of aerobraking into a near-polar two-hour orbit. This particular orbit provides up to 24 occultations of the atmosphere per sol. More details on the NOMAD and ACS spectrometer suites can be found in Vandaele et al. (2018) and Korablev et al. (2018) respectively. Both spectrometer suites can retrieve water vapour and temperature profiles up to around 100 km with typical vertical sampling of 1km spanning a wide range of local times and spatial locations. The differing boresights and sharing of occultations between the NOMAD and ACS instruments mean that the water vapour profile datasets generally alternate between different instruments, with data assimilation therefore providing an optimal way of unifying all separate observational datasets to create a global perspective of the vertical distribution of water that is not possible by any one instrument alone.

NOMAD/ACS water vapour profiles

Full details of the NOMAD SO (solar occultation) water vapour retrievals (in the spectral range from 2.3-4.3 μm) can be found in Aoki et al. (2019) and Villanueva et al. (2021). Measurements of diffraction order 134 and 168 are analysed, with both orders having strong H_2O bands. As the occultation profiles are restricted to the terminator, the local solar time is generally around 6 a.m. or 6 p.m. outside of the polar regions. Radiative transfer code is used to perform the retrieval using an 'onion peeling' method, with the retrieval starting at the top of the atmosphere (120 km) from an initial guess of the H2O volume mixing ratio (generally 1 ppm). Once a H_2O absorption feature is detected, the retrieved value is used as an initial guess for the layer below.

Solar occultations from the ACS NIR (near-infrared; 0.7-1.7 μm) spectrometer provide the water vapour vertical profile up to around 100 km with a resolution of 1-3 km, with full details in Fedorova et al. (2020). The retrieved volume fraction of water (i.e. mixing ratio) is deduced using established methods that include the extraction of the HO2 molecular abundance from the 1.38 μm absorption band. Spectra were fitted with a spectroscopic model at all altitudes below 100 km and the profiles of gaseous component are retrieved using an iterative algorithm. Water vapour vertical profiles have also been retrieved by the ACS MIR (mid-infrared) spectrometer (Alday et al. 2021; Olsen et al., 2021), with the ACS NIR and ACS MIR providing coincident profiles with good agreement (see supplementary material of Fedorova et al. (2020)). ACS MIR water vapour profiles are retrieved from spectra taken by the secondary grating position 4, 11 and 12 that cover absorption bands of several isotopologues of water vapour. Vertical profiles of pressure and temperature are retrieved from CO_2 absorption along with the H_2O volume mixing ratio. Figure 4 displays the spatiotemporal location of NOMAD SO, ACS NIR and ACS MIR water vapour profiles that are assimilated into the MGCM to form part of the final reanalysis product. During the time

period covered by the NOMAD and ACS instruments, 1,173 NOMAD and 2,381 ACS water vapour profiles are assimilated into the MGCM to produce the final reanalysis product.

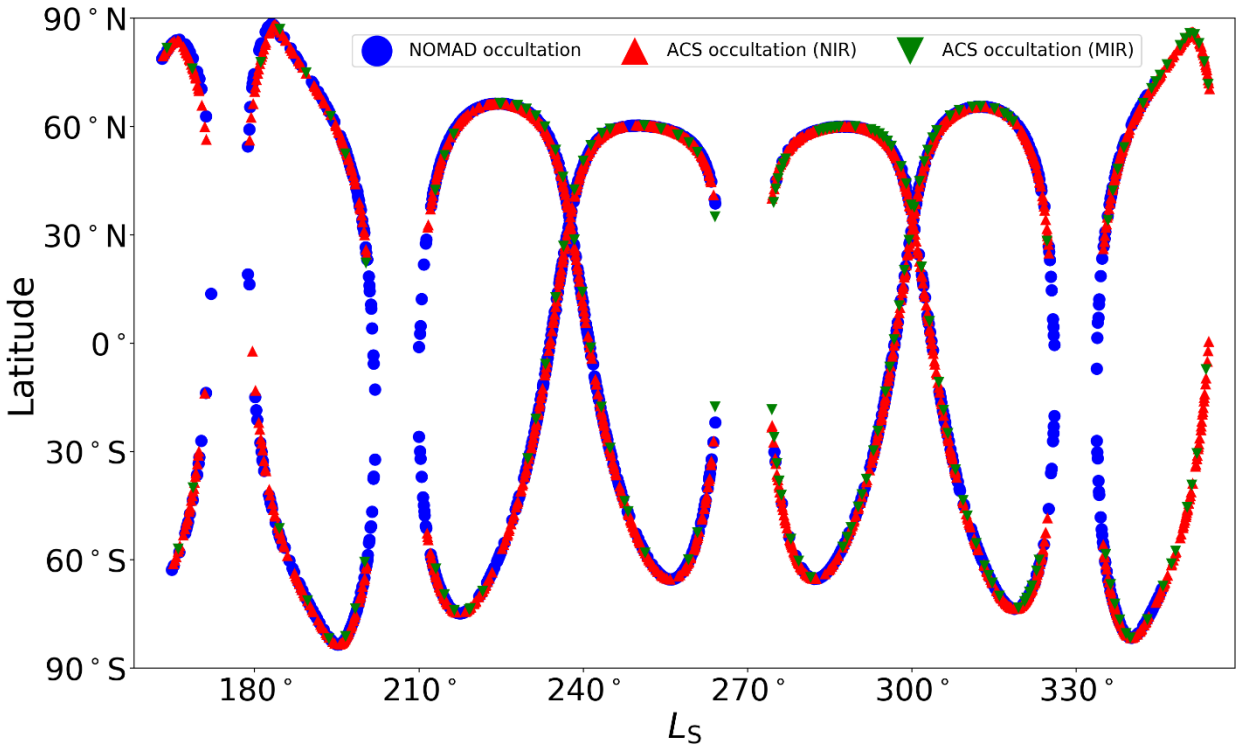

Figure 4- Spatio-temporal location of NOMAD SO (blue), ACS NIR (red) and ACS MIR (green) water vapour profiles.

NOMAD water vapour column

Retrievals of the water vapour column from the NOMAD instrument are fully detailed in Crismani et al. (2021). The observations are taken using the LNO (Limb Nadir and solar Occultation) spectrometer of NOMAD, covering the spectral range from 2.3-3.8 µm. Orders 167-169 of the Acousto-Optic Tunable Filter are used to retrieve the water vapour column with the effective resolving power of the instrument found to be 10,500. The retrievals are mainly dependent on the intensity of the narrow molecular absorptions in the flux ratio spectrum. The dataset samples local times from 8 a.m. to 4 p.m. and the geometry of the orbit allows for sampling in both hemisphere up to 75° latitude.

The retrievals are filtered to remove observations with a solar zenith angle greater than 60° and any retrievals for which the uncertainty on the retrieved molecular abundance is greater than the retrieved molecular abundance. Figure 5 displays the number of NOMAD LNO column water vapour retrievals that are assimilated into the MGCM to form part of the final reanalysis product. During the time period covered by the NOMAD LNO instrument, around 36,000 column water vapour retrievals are assimilated into the MGCM to produce the final reanalysis product.

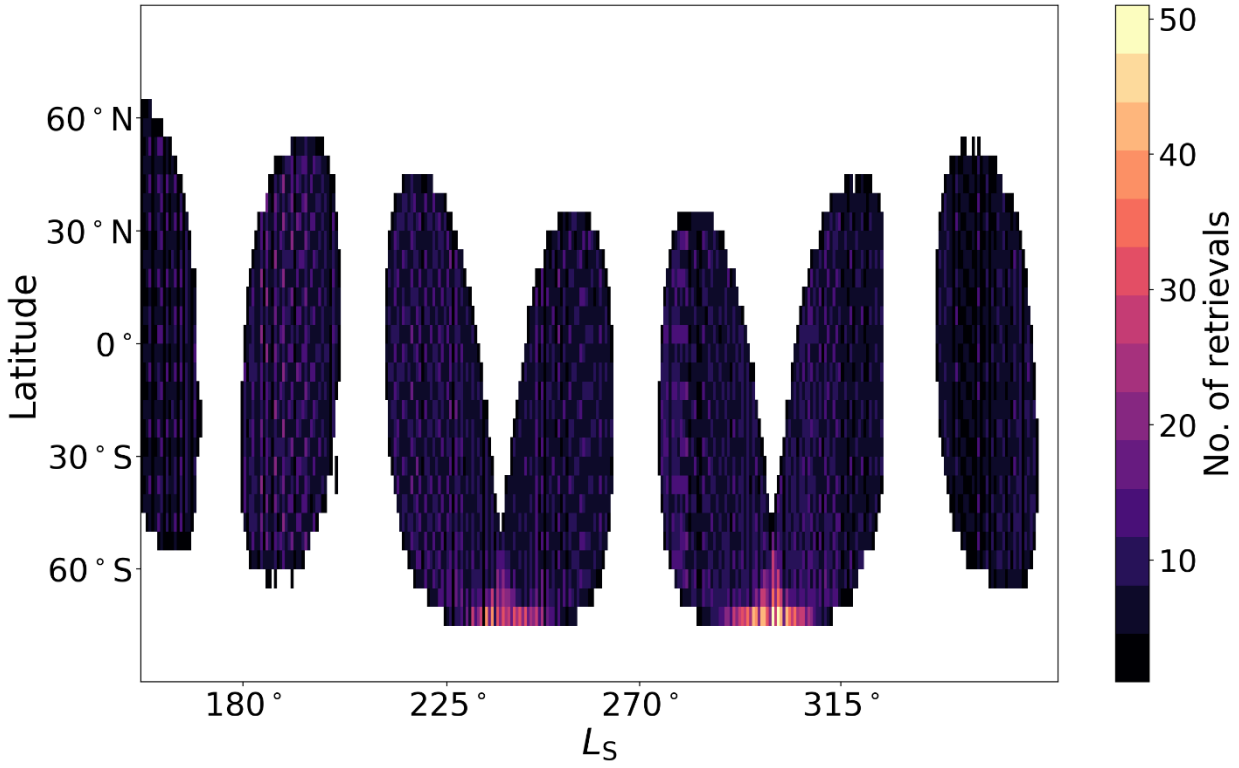

Figure 5 - Number of retrievals of NOMAD LNO column water vapour in 1 sol by 5˚ latitude bins. White indicates no data available in this particular bin.

ACS temperature profiles

Solar occultations from the ACS NIR spectrometer also provide the temperature vertical profile up to around 100 km with a resolution of 1-3 km, with full details in Fedorova et al. (2020). The temperature is retrieved using established methods that include the extraction of the CO_2 molecular abundance in the 1.57 µm absorption band. ACS NIR can resolve the spectral structure of the CO_2 rotational band therefore providing simultaneous temperature and pressure parameters self consistently.

Temperature profiles have also been retrieved by the ACS MIR spectrometer (Alday et al. 2021; Olsen et al., 2021), with the ACS NIR and ACS MIR providing coincident profiles with good agreement (see supplementary material of Fedorova et al. (2020)). Figure 6 displays the spatiotemporal location of ACS NIR and ACS MIR temperature profiles that are assimilated into the MGCM to form part of the final reanalysis product. During the time period covered by the ACS instrument, 1,507 ACS NIR and 572 ACS MIR temperature profiles are assimilated into the MGCM to produce the final reanalysis product.

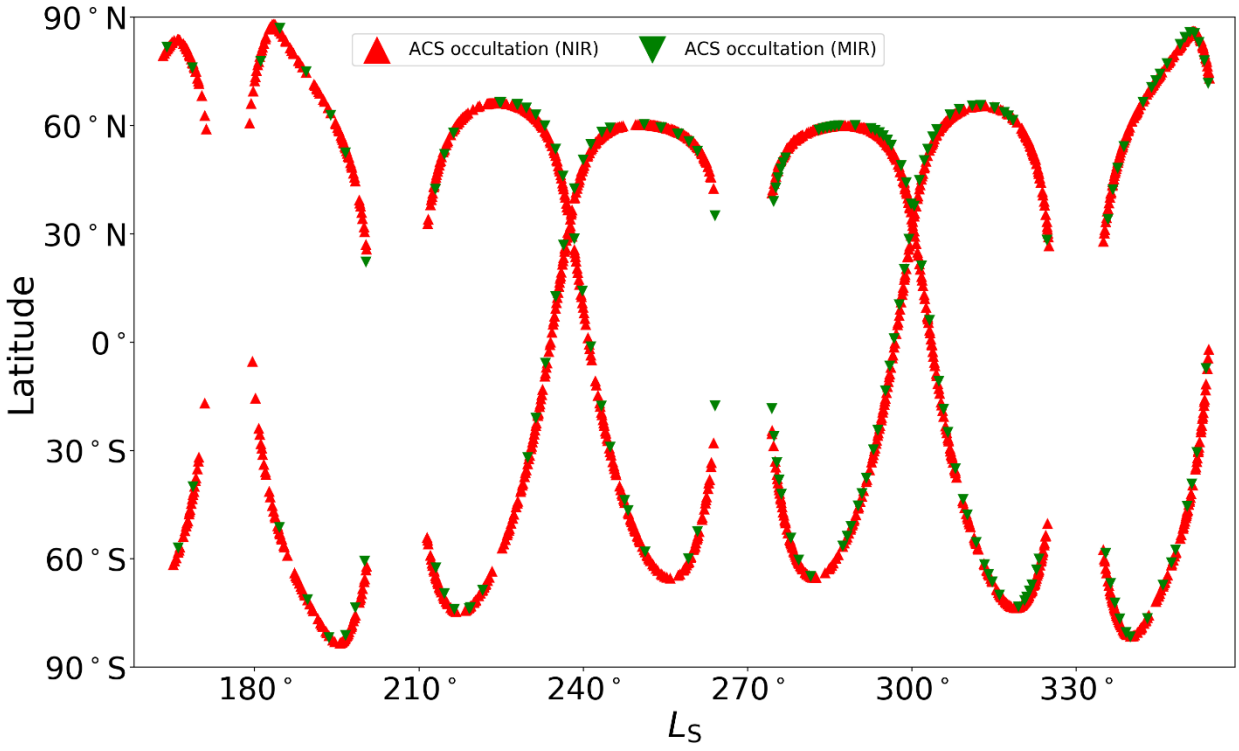

Figure 6 – Spatio-temporal location of ACS NIR (red) and ACS MIR (green) temperature profiles.

Data assimilation scheme

To assimilate the observations, the MGCM uses the Analysis Correction (AC) scheme (Lorenc et al., 1991) adapted to Martian conditions. The AC scheme has previously been used to assimilate thermal and dust opacity retrievals from TES (Lewis & Barker, 2005) which are used to indirectly study the thermal tides. The dust opacity retrievals have also been used to perform a multi-annual study of interannual dust variability (Montabone et al., 2005, 2015), indicating localised regions which triggered the onset of the global dust storm in MY 25 and also found dust lifting by dust devils to contribute little. Observations during the TES aerobraking phase have been assimilated indicating an atmospheric warming at the onset of northern hemisphere winter due to the dust storm in MY 23 (Lewis et al., 2007). The AC scheme has also been validated against radio occultation (RO) measurements (Montabone et al., 2006), with the assimilation of TES thermal and dust opacity retrievals improving the agreement between the MGCM and the RO profiles. Recent work with the AC scheme has moved on to the assimilation of chemically passive water vapour and water ice (Steele et al., 2014a,b) to investigate the Martian water cycle and radiative effect of water ice clouds respectively and chemically active species such as ozone (Holmes et al., 2018) and carbon monoxide (Holmes et al., 2019).

The AC scheme is a form of successive corrections in which analysis steps are interleaved with each model dynamical time step. The modified successive corrections equation used by the scheme is

$$\mathbf{x}_a = \mathbf{x}_b + \mathbf{WQ}[\mathbf{y}_o\text{-}H(\mathbf{x}_b)]$$

where $\mathbf{x}_a$ is the analysis vector, $\mathbf{x}_b$ is the model background, $\mathbf{y}_o$ is the observation vector, H is the observation operator and **W** and **Q** are matrices of weights and normalization factors respectively. In each analysis step, the above equation is split into separate vertical and horizontal stages in order to spread the analysis increments from the observation locations to the surrounding model grid

points. This is followed by the derivation of multi-variate increment fields for dynamical balance where applicable (e.g. after assimilating temperatures, geostrophic wind adjustments are applied).

Observations are inserted over an asymmetrical specified time window of 6 hours (five hours before an observations valid time until one hour after), optimally selected so that the assimilation will not unrealistically smooth out any inherent model variation. The asymmetrical time window is also used as it is beneficial because it biases the assimilation gains to regions ahead of the satellite ground track, which have not recently been observed. Spreading in time was also found to be beneficial in the case of relatively sparse data, where it is often better to use an observation from a slightly different time, with a reduced weight, rather than release the model which would then quickly relax back toward a temperature determined principally by its dust distribution, since the radiative timescale of the Martian atmosphere is only 1–2 sols.

Acknowledgments

This project has received funding from the UK Space Agency under grant numbers ST/R001405/1 and ST/W00268X/1.

References

Alday, J., Trokhimovskiy, A., Irwin, P. G. J., Wilson, C. F., Montmessin, F., Lefèvre, F., ... Shakun, A. (2021). Isotopic fractionation of water and its photolytic products in the atmosphere of Mars. *Nature Astronomy*, 5, 943-950.

Aoki, S., Vandaele, A. C., Daerden, F., Villanueva, G. L., Liuzzi, G., Thomas, I. R., ... Lopez-Moreno, J. J. (2019). Water Vapor Vertical Profiles on Mars in Dust Storms Observed by TGO/NOMAD. *J. Geophys. Res. (Planets),* 124 (12), 3482-3497.

Colaïtis, A., Spiga, A., Hourdin, F., Rio, C., Forget, F., and Millour, E. (2013). A thermal plume model for the Martian convective boundary layer. *J. Geophys. Res.: Planets*, 118: 1468-1487.

Crismani, M. M. J., Villanueva, G. L., Liuzzi, G., Smith, M. D., Knutsen, E. W., ... Vandaele, A. C. (2021). A global and seasonal perspective of martian water vapor from ExoMars/NOMAD. *J. Geophys. Res. (Planets),* 126 (11), e2021JE006878.

Fedorova, A., Montmessin, F., Korablev, O., Luginin, M., Trokhimovskiy, A., Belyaev, D. A., ... Wilson, C. F. (2020). Stormy water on Mars: The distribution and saturation of atmospheric water during the dusty season. *Science*,758 367 (6475), 297-300.

Holmes, J. A., Lewis, S. R., Patel, M. R., and Lefèvre, F. (2018). A reanalysis of ozone on Mars from assimilation of SPICAM observations. *Icarus*, 302, 308-318.

Holmes, J. A., Lewis, S. R., Patel, M. R., & Smith, M. D. (2019). Global analysis and forecasts of carbon monoxide on Mars. *Icarus,* 328, 232-245.

Kleinböhl, A., Schofield, J. T., Kass, D. M., Abdou, W. A., Backus, C. R., Sen, B., Shirley, J. H., Lawson, W. G., Richardson, M. I., Taylor, F. W., Teanby, N. A., and McCleese, D. J. (2009). Mars Climate Sounder limb profile retrieval of atmospheric temperature, pressure, and dust and water ice opacity. *J. Geophys. Res.: Planets*, 114 (E10006): 1-30.

Kleinböhl, A., Friedson, A. J., & Schofield, J. T. (2017). Two-dimensional radiative transfer for the retrieval of limb emission measurements in the martian atmosphere. *J. Quant. Spectrosc. Ra.*, 187, 511-522.

Kleinböhl, A., Spiga, A., Kass, D. M., Shirley, J. H., Millour, E., Montabone, L., & Forget, F. (2020). Diurnal Variations of Dust During the 2018 Global Dust Storm Observed by the Mars Climate Sounder. *J. Geophys. Res. (Planets)*, 125 (1), e06115.

Korablev, O., Montmessin, F., Trokhimovskiy, A., Fedorova, A. A., Shakun, A. V., Grigoriev, A. V., ... Zorzano, M. P. (2018). The Atmospheric Chemistry Suite (ACS) of Three Spectrometers for the ExoMars 2016 Trace Gas Orbiter. *Space Science Reviews*, 214 (1), 7.

Lefèvre, F., Bertaux, J.-L., Clancy, R.T., Encrenaz, T., Fast, K., Forget, F., Lebonnois, S., Montmessin, F., Perrier, S. (2008). Heterogeneous chemistry in the atmosphere of Mars. *Nature,* 454, 971–975.

Lefèvre, F., Lebonnois, S., Montmessin, F., Forget, F. (2004). Three-dimensional modeling of ozone on Mars*. J. Geophys. Res.* 109, 7004.

Lewis, S. R., and Barker, P. R. (2005). Atmospheric tides in a Mars general circulation model with data assimilation. *Adv. Space Res.*, 36: 2162-2168.

Lewis, S. R., Read, P. L., Conrath, B. J., Pearl, J. C., and Smith, M. D. (2007). Assimilation of thermal emission spectrometer atmospheric data during the Mars Global Surveyor aerobraking period. *Icarus*, 192: 327-347.

Lorenc, A. C., Bell, R. S., and MacPherson, B. (1991). The Meteorological Office analysis correction data assimilation scheme. *Quart. J. Royal Meteorol. Soc.*, 117: 59-89.

Madeleine, J.-B., Forget, F., Millour, E., Montabone, L., and Wolff, M. J. (2011). Revisiting the radiative impact of dust on Mars using the LMD Global Climate Model. *J. Geophys. Res.*, 116(E11010): 1-13.

McCleese, D. J., Schofield, J. T., Taylor, F. W., Calcutt, S. B., Foote, M. C., Kass, D. M., Leovy, C. B., Paige, D. A., Read, P. L., and Zurek, R. W. (2007). Mars Climate Sounder: An investigation of thermal and water vapor structure, dust and condensate distributions in the atmosphere, and energy balance of the polar regions. *J. Geophys. Res.: Planets*, 112(E05S06): 1-16.

Montabone, L., Lewis, S. R., and Read, P. L. (2005). Interannual variability of Martian dust storms in assimilation of several years of Mars global surveyor observations. *Adv. Space Res.*, 36: 2146-2155.

Montabone, L., Lewis, S. R., Read, P. L., and Hinson, D. P. (2006). Validation of martian meteorological data assimilation for MGS/TES using radio occultation measurements. *Icarus*, 185: 113-132.

Montabone, L., Marsh, K., Lewis, S. R., Read, P. L., Smith, M. D., Holmes, J., Spiga, A., Lowe, D., and Pamment, A. (2014). The Mars Analysis Correction Data Assimilation (MACDA) Dataset V1.0. *Geosci. Data J.*, 1(2): 129-139.

Montabone, L., Forget, F., Millour, E., Wilson, R. J., Lewis, S. R., Cantor, B. A., Kass, D., Kleinböhl, A., Lemmon, M. T., Smith. M. D., and Wolff, M. J. (2015). Eight year climatology of dust optical depth on Mars. *Icarus*, 251: 65-95.

Navarro, T., Madeleine, J.-B., Forget, F., Spiga, A., Millour, E., Montmessin, F., & Määttänen, A. (2014). Global climate modeling of the Martian water cycle with improved microphysics and radiatively active water ice clouds. *Journal of Geophysical Research (Planets),* 119, 1479-1495.

Newman, C. E., Lewis, S. R., Read, P. L., and Forget, F. (2002). Modeling the Martian dust cycle, 1. Representations of dust transport processes. *J. Geophys. Res.*, 107(E12): 1-18.

Olsen, K. S., Trokhimovskiy, A., Montabone, L., Fedorova, A. A., Luginin, M., Lefèvre, F., ... Shakun, A. (2021). Seasonal reappearance of HCl in the atmosphere of Mars during the Mars year 35 dusty season. *Astron. Astrophys.*, 647, A161.

Priestley, A. (1993). A quasi-conservative version of the semi-lagrangian advection scheme. *Mont. Weath. Rev.*, 121: 621-629.

Steele, L. J., Lewis, S. R., and Patel, M. R. (2014a). The radiative impact of water ice clouds from a reanalysis of Mars Climate Sounder data. *Geo. Res. Lett.*, 41: 4471-4478.

Steele, L. J., Lewis, S. R., Patel, M. R., Montmessin, F., Forget, F., and Smith, M. D. (2014b). The seasonal cycle of water vapour on Mars from assimilation of Thermal Emission Spectrometer data. *Icarus*, 237: 97-115.

Vandaele, A. C., Lopez-Moreno, J. J., Patel, M. R., Bellucci, G., Daerden, F., Ristic, B., … Wolff, M. (2018). NOMAD, an Integrated Suite of Three Spectrometers for the ExoMars Trace Gas Mission: Technical Description, Science Objectives and Expected Performance. *Space Science Reviews*, 214 (5), 80.

Villanueva, G. L., Liuzzi, G., Crismani, M. M. J., Aoki, S., Vandaele, A. C., ... NOMAD team. (2021). Water heavily fractionated as it ascends on Mars as revealed by ExoMars/NOMAD. *Science Advances*, 7 (7).